Vibrational transition moments of CH_4 from first principles

Sergei N. Yurchenko*, Jonathan Tennyson, Robert J. Barber

Department of Physics and Astronomy, University College London, London, WC1E 6BT, UK

Walter Thiel

Max-Planck-Institut für Kohlenforschung, Kaiser-Wilhelm-Platz 1, D–45470 Mülheim an der Ruhr, Germany

Abstract

A new nine-dimensional (9D), *ab initio* electric dipole moment surface (DMS) of methane in its ground electronic state is presented. The DMS is computed using an explicitly correlated coupled cluster CCSD(T)-F12 method in conjunction with an F12-optimized correlation consistent basis set of the TZ-family. A symmetrized molecular bond representation is used to parameterise the 9D DMS in terms of sixth-order polynomials. Vibrational transition moments as well as band intensities for a large number of IR-active vibrational bands of $^{12}CH_4$ are computed by vibrationally averaging the *ab initio* dipole moment components. The vibrational wavefunctions required for these averages are computed variationally using the program TROVE and a new 'spectroscopic' $^{12}CH_4$ potential energy surface. The new DMS will be used to produce a hot line list for $^{12}CH_4$.

Keywords: Methane, dipole moment, IR, transition dipole, vibration, CH4, intensity, variational calculations, DMS, PES

*Corresponding author

Email addresses: s.yurchenko@ucl.ac.uk (Sergei N. Yurchenko), j.tennyson@ucl.ac.uk (Jonathan Tennyson), rjb@star.ucl.ac.uk (Robert J. Barber), thiel@mpi-muelheim.mpg.de (Walter Thiel)

1. Introduction

Methane plays an important role in atmospheric and astrophysical chemistry. Its rotation-vibration spectrum is of key importance for models of the atmospheres of bodies ranging from Titan to cool stars. However the lack of precise data on methane spectra, particularly at higher temperatures, has severely limited models for atmospheres as diverse as Jupiter [1], exoplanets [2, 3] and brown dwarfs [4]. Any temperature-dependent model of the methane spectrum requires a reliable treatment of the associated transition intensities. The construction of a reliable electric dipole moment surface (DMS) which can be used to generate such intensities concerns us in this paper.

Theoretically, a number of *ab initio* potential energy surfaces (PES) computed at different levels of theory have been reported [5–10]. The surface by Schwenke and Partridge [7] has been used in many benchmark studies as well as for accurate predictions of vibrational and ro-vibrational energies of CH_4. However, to our knowledge no accurate and comprehensive *ab initio* DMSs of CH_4 have been published so far. In some cases *ab initio* DMSs were used, but not actually provided, for example by Oyanagi et al. [9] (at the CCSD(T)/cc-pVTZ and MP2/cc-pVTZ level of theory) and Warmbier et al. [11] (RCCSD(T)/aug-cc-pVTZ). An empirical DMS of limited accuracy was developed by Hollenstein et al. [12].

The goal of this paper is to bridge this gap and provide an accurate and detailed *ab initio* DMS of CH_4. To this end we employed an explicitly correlated (F12) coupled cluster method in conjunction with an F12-optimized basis set to generate a nine-dimensional (9D) DMS of CH_4. This surface is then used to compute vibrational transition moments and vibrational band intensities of $^{12}CH_4$ for a large number of IR-active transitions in the range between 0 and 10000 cm^{-1}. This is done by vibrationally averaging the DMS over vibrational functions of $^{12}CH_4$ computed through variationally solving the nuclear motion Schrödinger equation with the TROVE program [13]. This program has been used successfully for accurate and extensive ro-vibrational calculations on different tetratomic molecules [14–21]. The present work is the first application of TROVE to a larger system. Other variational approaches capable of treating this pentatomic molecule include the Lanczos-method developed by Carrington and Wang [22–25], MULTIMODE [26–29], and GENIUSH [30] as well as the methods of Halonen [31], Xie and Tennyson [32], Schwenke [33], and Nikitin [34]. The rigorous quantum dynamics algorithm employed by Yu [35, 36] should be also mentioned as an alternative accurate approach employed for calculating vibrational energies of CH_4.

On the experimental side, electric transition dipole moments for CH_4 are the subject of a large number of publications [37–47], where effective dipole moment parameters were derived

either through fits to intensity measurements or using perturbation theory. The most recent and comprehensive collection of the effective dipole moment parameters describing excitations in the region up to 4800 cm^{-1} was reported recently by Albert et al. [47]. Many of these studies also provide band intensities. We use some of these data to validate our vibrational transition moments as well as our DMS, where possible.

The paper is structured as follows. In Section 2 the *ab initio* method used for generating DMS of CH_4 is described and an analytical representation for this DMS is introduced. The PES is detailed in Section 3. The variational approach is described in Section 4 and theoretical vibrational transition moments and band intensities are reported in Section 5. Finally, Section 6 offers some discussion and future prospects.

2. Ab initio calculations

We used the recently proposed explicitly correlated F12 coupled cluster method with single and double excitations including a perturbational estimate of connected triple excitations, CCSD(T)-F12c [48] in conjunction with the corresponding F12-optimized correlation-consistent basis sets, namely aug-cc-pVTZ-F12 [49] (augmented correlation-consistent polarized valence triple-zeta basis) as implemented in Molpro 2010 [50].

Methane has nine vibrational degrees of freedom and thus requires a very extensive grid of geometries in the *ab initio* calculations. We have computed three *ab initio* DMSs (one for each Cartesian component) on a fine grid of 114,000 geometries covering the energy range up to 50,000 cm^{-1} with C–H distances ranging from 0.75 to 2.0 Å, and interbond angles ranging from 50 to 140°. The finite field method, with a field of 0.005 a.u., was used to compute the dipole moment component as first derivatives with respect to the external electric field in the dipole approximation.

In order to represent the *ab initio* dipole moment vector $\vec{\mu}$ of CH_4 analytically we use the so-called symmetrized molecular bond (SMB) representation [8], where $\vec{\mu}$ is projected onto three symmetrized combinations of vectors associated with the four molecular bonds C-H_i ($i = 1, 2, 3, 4$). An analogous approach was used to represent the *ab initio* dipole moment of NH_3 [51] (see also Ref. [8] for a non-symmetrized MB representation of the methane DMS). The three components of the dipole moment of CH_4 span three components of the F_2 representation, i.e. F_{2x}, F_{2y}, and F_{2z} in the irreducible representation of the T_d(M) molecular symmetry group [52]. We define the following three symmetrically independent reference vectors $\vec{n}_\Gamma$ spanning the same

representation F_2:

$$\vec{n}_{F_{2x}} = \frac{1}{2}\left(\frac{\vec{r}_1}{|\vec{r}_1|} - \frac{\vec{r}_2}{|\vec{r}_2|} + \frac{\vec{r}_3}{|\vec{r}_3|} - \frac{\vec{r}_4}{|\vec{r}_4|}\right), \tag{1}$$

$$\vec{n}_{F_{2y}} = \frac{1}{2}\left(\frac{\vec{r}_1}{|\vec{r}_1|} - \frac{\vec{r}_2}{|\vec{r}_2|} - \frac{\vec{r}_3}{|\vec{r}_3|} + \frac{\vec{r}_4}{|\vec{r}_4|}\right), \tag{2}$$

$$\vec{n}_{F_{2z}} = \frac{1}{2}\left(\frac{\vec{r}_1}{|\vec{r}_1|} + \frac{\vec{r}_2}{|\vec{r}_2|} - \frac{\vec{r}_3}{|\vec{r}_3|} - \frac{\vec{r}_4}{|\vec{r}_4|}\right), \tag{3}$$

where $\vec{r}_i$ is a molecular bond vector pointing from C to H_i ($i = 1, 2, 3, 4$). The dipole moment vector $\vec{\mu}$ can now be represented as

$$\vec{\mu} = \vec{n}_{F_{2x}}\mu_{F_{2x}} + \vec{n}_{F_{2y}}\mu_{F_{2y}} + \vec{n}_{F_{2z}}\mu_{F_{2z}}, \tag{4}$$

where the projections $\mu_{F_{2\alpha}}$ ($\alpha = x, y, z$) are the dipole moment functions also spanning the F_2 representation. Each component $\mu_{F_{2\alpha}}$ is then expanded as

$$\mu_{F_{2\alpha}} = \sum_{i_1,i_2,\ldots,i_9} \mu^{\alpha}_{i_1,i_2,\ldots,i_9} \xi_1^{i_1}\xi_2^{i_2}\ldots\xi_9^{i_9}, \tag{5}$$

in terms of the following set of nine independent internal coordinates:

$$\xi_i = (r_i - r_e)\, e^{-\beta(r_i - r_e)^2}, \quad i = 1, 2, 3, 4, \tag{6}$$

$$\xi_5 = \frac{1}{\sqrt{12}}(2\alpha_{12} - \alpha_{13} - \alpha_{14} - \alpha_{23} - \alpha_{24} + 2\alpha_{34}), \tag{7}$$

$$\xi_6 = \frac{1}{2}(\alpha_{13} - \alpha_{14} - \alpha_{23} + \alpha_{24}), \tag{8}$$

$$\xi_7 = \frac{1}{\sqrt{2}}(\alpha_{24} - \alpha_{13}), \tag{9}$$

$$\xi_8 = \frac{1}{\sqrt{2}}(\alpha_{23} - \alpha_{14}), \tag{10}$$

$$\xi_9 = \frac{1}{\sqrt{2}}(\alpha_{34} - \alpha_{12}), \tag{11}$$

where r_i are the bond lengths and α_{ij} are the interbond angles. Following Hollenstein *et al.* [12], we have introduced the factor $\exp\left(-\beta(r_i - r_e)^2\right)$ in order to keep the expansion in Eq. (5) from diverging at large r_i. Here r_e is a reference expansion center which is conveniently taken at a value close to the molecular equilibrium.

The properties of the components $\mu_{F_{2\alpha}}$ associated with F_2 impose symmetry relations between the expansion coefficients $\mu^{\alpha}_{i_1,\ldots,i_9}$. These relations can be reconstructed by applying the standard symmetry transformation rules [52, 53] between the F_{2x}, F_{2y}, F_{2z} components of F_2. We employed the Maple program function 'solve' to find a set of independent coefficients $\mu^{\alpha}_{i_1,\ldots,i_9}$ by solving an over-determined system of linear equations (see Ref. [54] for details on the computational procedure). For example, to first order the dipole moment functions μ_α are given by

the expansions

$$\mu_{F_{2x}} = \mu_7\xi_7 + \mu_1(\xi_1 - \xi_2 + \xi_3 - \xi_4) + O(\xi_k^2)\ldots, \quad (12)$$

$$\mu_{F_{2y}} = \mu_7\xi_8 + \mu_1(\xi_1 - \xi_2 - \xi_3 + \xi_4) + O(\xi_k^2)\ldots, \quad (13)$$

$$\mu_{F_{2z}} = \mu_7\xi_9 + \mu_1(\xi_1 + \xi_2 - \xi_3 - \xi_4) + O(\xi_k^2)\ldots, \quad (14)$$

where the shorthand notations $\mu_7 = \mu^{\alpha}_{0,0,0,0,0,0,1,0,0}$ and $\mu_1 = \mu^{\alpha}_{1,0,0,0,0,0,0,0,0}$ are used. The complete expansion set is given in the supplementary material to this paper. A full sixth-order symmetrized expansion requires 680 symmetrically independent dipole moment parameters in total. Taking into account the symmetry relations, the expansion Eq. (5) can be written as:

$$\mu_\alpha = \sum_{i_1,i_2,\ldots,i_9} \mu^{\alpha}_{i_1,i_2,i_3,\ldots,i_9} \{\xi_1^{i_1}\xi_2^{i_2}\ldots\xi_9^{i_9}\}^{F_{2\alpha}}, \quad (15)$$

where $\{\xi_1^{i_1}\xi_2^{i_2}\ldots\xi_9^{i_9}\}^{F_{2\alpha}}$ is a symmetrized combination of different permutations of the internal coordinates consistent with $T_{\mathrm{d}}(\mathrm{M})$ group operations and spanning the $F_{2\alpha}$ symmetry.

The actual values of expansion parameters $\mu^{\alpha}_{i_1,i_2,i_3,\ldots,i_9}$ corresponding to our *ab initio* DMS were determined through least-squares fittings to the 114,000 *ab initio* dipole moment values. Some parameters with large standard errors that exhibit strong correlation were constrained to zero. The *ab initio* data in these fits were weighted using the following expression proposed by Partridge and Schwenke [55]:

$$w_i = N\frac{\tanh\left[-0.0004\ \mathrm{cm}\times\left(V_i - 18\,000\ \mathrm{cm}^{-1}\right)\right] + 1.00000002}{2.00000002}, \quad (16)$$

where N is a normalization factor defined by $\sum_i w_1 = 1$ and V_i is the corresponding *ab initio* energy at the ith geometry (in cm^{-1}), measured relative to the equilibrium energy and computed using the same level of theory. The *ab initio* energy V_i is weighted by the factor w_i in the PES fitting; these weight factors favour the energies below 18 000 cm^{-1}. In the end 296 parameters were needed to obtain a weighted (w_i) root-mean-squares (rms) error of 0.00016 D. The expansion parameters are given in the supplementary materials of the paper along with a fortran 95 routine incorporating the corresponding analytical form.

3. Potential energy surface

In this work we use a new 'spectroscopic' PES generated as follows. First, an *ab initio* PES was generated on the same grid of 114,000 geometries employing the same CCSD(T)-F12c approach [48] as for the DMS, but with the larger aug-cc-pVQZ-F12 basis set [49]. The frozen core approximation was applied in the coupled cluster calculations. We did not include core-valence corrections and higher-order coupled cluster corrections because they cancel to a large

extent (see the work by Yachmenev et al. [18]), and also because this would be very costly with the resources available to us. Relativistic corrections were computed using the Douglas-Kroll method as implemented in Molpro 2010. With this method we obtained the equilibrium bond length $r_e = 1.08734$ Å, which is close to the value $r_e = 1.08595$ Å derived in a combined experimental/*ab initio* analysis [56]. The *ab initio* potential energies have been represented using a symmetrized analytical expansion in terms of the four stretching coordinates $1 - \exp(-a(r_i - r_e))$ $(i = 1, 2, 3, 4)$ and five bending coordinates ξ_j $(j = 5, 6, 7, 8, 9)$ from Eqs. (6–11). The symmetry relations between potential parameters in the T_d(M) group were derived employing Maple with the procedure described above. In total 287 symmetrically independent parameters are needed for a full sixth-order expansion. These expansion parameters were obtained from a fitting procedure using the weighting scheme given in Eq. (16). Some parameters showing large standard errors were constrained to zero, which resulted in 268 potential parameters needed to get a weighted rms error of 0.3 cm^{-1}.

To improve the quality of the *ab initio* PES, we slightly refined it by fitting to the 'experimental' energies of $^{12}CH_4$ extracted from the HITRAN 2008 [57] database for $J = 0, 1, 2, 3, 4$. In these fittings the variational program TROVE [13] was used, closely following the approach described in detail by Yurchenko et al. [58]. This new 'spectroscopic' PES for $^{12}CH_4$ will be the subject of further improvements and a future publication. Both the initial *ab initio* and refined potential parameters are given as supplementary material along with a fortran 95 program containing the corresponding potential energy function.

4. Variational calculations

The vibrational wavefunctions and energies of $^{12}CH_4$ were calculated using the variational program TROVE [13]. In this approach the Hamiltonian operator is represented as an expansion around a reference geometry taken presently at the molecular equilibrium. The kinetic energy operator is expanded in terms of the nine linearized coordinates ξ_i^ℓ, which are linearized versions of the internal coordinates ξ_i $(i = 1, \ldots, 9)$ defined above; for the potential energy function we use $1 - \exp(-a\xi_i^\ell)$ $(i = 1, 2, 3, 4)$ for the four stretching and ξ_j^ℓ $(j = 5, 6, 7, 8, 9)$ for the five bending linearized coordinates. The latter expansions were applied to the refined PES introduced above. The kinetic and potential energy parts were truncated after the sixth and eighth order, respectively.

To construct the basis set, TROVE employs a multi-step contraction scheme based on the following polyad truncation. The polyad number in case of CH_4 is given by

$$P = 2(v_1 + v_2 + v_3 + v_4) + v_5 + v_6 + v_7 + v_8 + v_9, \tag{17}$$

where v_i is a vibrational quantum number associated with a one-dimensional primitive basis function $\phi_{v_i}(\xi_i^\ell)$ $(i = 1, 2, 3, \ldots, 9)$. At Step 1, nine sets of $\phi_{v_i}(\xi_i^\ell)$ are generated using the Numerov-Cooley [59, 60] method by solving the 1D Schrödinger equations for each of the nine modes separately. The corresponding 1D Hamiltonian operators are obtained from the 9D Hamiltonian operator ($J = 0$) by freezing all but one vibrational coordinates at their equilibrium values. At Step 2 the 9D coordinate space is divided into the three reduced sub-spaces, (i) $\{\xi_1^\ell, \xi_2^\ell, \xi_3^\ell, \xi_4^\ell\}$, (ii) ξ_5^ℓ, ξ_6^ℓ, and (iii) $\xi_7^\ell, \xi_8^\ell, \xi_9^\ell$. This division is dictated by symmetry: each of the sub-spaces is symmetrically independent and thus can be processed separately. For each of these sub-spaces, the Schrödinger equations are solved for the corresponding reduced Hamiltonian operators employing as basis the products of the corresponding primitive functions $\phi_{v_i}(\xi_i^\ell)$ generated at Step 1. The sub-space bases are truncated using the condition $P \leq P_{\max}$, where P is given by Eq. (17). In this work we use $P_{\max} = 12$, i.e. our reduced sub-space basis sets are defined by

$$v_1 + v_2 + v_3 + v_4 \leq 6, \tag{18}$$

$$v_5 + v_6 \leq 12, \tag{19}$$

$$v_7 + v_8 + v_9 \leq 12. \tag{20}$$

The three sets of eigenfunctions $\Psi_{\lambda_1}^{(\mathrm{i})}(\xi_1^\ell, \xi_2^\ell, \xi_3^\ell, \xi_4^\ell)$, $\Psi_{\lambda_2}^{(\mathrm{ii})}(\xi_5^\ell, \xi_6^\ell)$, and $\Psi_{\lambda_3}^{(\mathrm{iii})}(\xi_7^\ell, \xi_8^\ell, \xi_9^\ell)$ resulting from these solutions are symmetrized and assigned local mode quantum numbers (i) v_1, v_2, v_3, v_4, (ii) v_5, v_6, and (iii) v_7, v_8, v_9 and vibrational symmetry Γ_{vib}. The final vibrational basis set is formed from products $\Psi_{\lambda_1}^{(\mathrm{i})} \times \Psi_{\lambda_2}^{(\mathrm{ii})} \times \Psi_{\lambda_3}^{(\mathrm{iii})}$, which are contracted with $P \leq 12$ and symmetrized again using the standard technique for transformations to irreducible representations (see, for example, Ref. [52]). Thus our contracted vibrational basis set consists of ten symmetrically independent groups, one for each irreducible representation of the $T_{\mathrm{d}}(\mathrm{M})$ group A_1, A_2, E_a, E_b, F_{1x}, F_{1y}, F_{1z}, F_{2x}, F_{2y}, F_{2z}. From the degenerate symmetries E, F_1, and F_2, only the first component is processed. Therefore only five vibrational Hamiltonian matrices (one for each symmetry) are constructed and diagonalized. In the diagonalizations we use the eigensolver DSYEV from LAPACK as implemented in the MKL libraries. The dimensions of the matrices to be diagonalized are 2190, 1725, 3901, 5481, and 5940 for A_1, A_2, E, F_1, and F_2, respectively. The results are collected in Tables 1–3, where the calculated energies are also compared with the available experimental values from [47, 61–63]. It should be noted that our basis set with $P \leq 12$ does not provide fully converged energies. The same comment applies to our new 'spectroscopic' PES: because of the limitations of the method, this PES can only guarantee the energies given in Table 1 when used with the same approach and basis set employed in the refinements, i.e.

$P_{\max} = 12$. However the vibrational transition moments reported in the next section appear to be rather insensitive to the size of the basis set and the shape of the potential.

5. Transition moments

The transition moment connecting two states i ('initial') and f ('final') can be defined as the vibrational average of a dipole moment component μ_α ($\alpha = x, y, z$):

$$\bar{\mu}_\alpha^{(i,\Gamma'_a;f,\Gamma''_b)} = \langle \Psi_i^{\Gamma'_a} | \mu_\alpha | \Psi_f^{\Gamma''_b} \rangle, \tag{21}$$

where μ_α ($\alpha = x, y, z$) are the Cartesian components of the dipole moment in the molecule-fixed frame (defined in TROVE by the Eckart conditions [64]); $\Psi_i^{\Gamma'_a}$ and $\Psi_f^{\Gamma''_b}$ are vibrational eigenfunctions obtained variationally, and Γ_s represents a component of one of the ten irreducible representations A_1, A_2, E_a, E_b, F_{1x}, F_{1y}, F_{1z}, F_{2x}, F_{2y}, F_{2z} of $T_{\rm d}$(M). It should be noted that the transition moments defined by Eq. (21) depend on the choice of the molecular-fixed coordinate system [65] as well as on the particular choice of the transformational properties of the irreducible representations E, F_1, and F_2 (we use irrep-matrices from Hougen's monograph [66]). The following quantity, averaged over the Cartesian components $\alpha = x, y, z$ and any degenerate components of the wavefunctions, is independent of these choices:

$$\bar{\mu}^{if} \equiv \bar{\mu}^{(i,\Gamma';f,\Gamma'')} = \sqrt{\left[\bar{\mu}_x^{(i,\Gamma';f,\Gamma'')}\right]^2 + \left[\bar{\mu}_y^{(i,\Gamma';f,\Gamma'')}\right]^2 + \left[\bar{\mu}_z^{(i,\Gamma';f,\Gamma'')}\right]^2}, \tag{22}$$

where

$$\bar{\mu}_\alpha^{(i,\Gamma';f,\Gamma'')} = \sum_{a,b} \bar{\mu}_\alpha^{(i,\Gamma'_a;f,\Gamma''_b)}, \tag{23}$$

and the vibrational transition moment $\bar{\mu}^{if}$ is defined as the length of the vector $\left[\bar{\mu}_x^{(i,\Gamma';f,\Gamma'')}, \bar{\mu}_y^{(i,\Gamma';f,\Gamma'')}, \bar{\mu}_z^{(i,\Gamma';f,\Gamma'')}\right]$.

A number of calculated values of the vibrational transition moments $\bar{\mu}^{if}$ as well as matrix elements $\bar{\mu}_x^{(i,\Gamma';f,\Gamma'')}$ of $^{12}CH_4$ corresponding to transitions from the three lowest vibrational states (ν_0, ν_2, and ν_4) are listed in Tables 1–3. The non-zero matrix elements $\bar{\mu}_x^{(i,\Gamma';f,\Gamma'')}$ in Tables 1–3 for each transition satisfy the following set of relations:

$$\begin{array}{llllllll}
\bar{\mu}_x^{(A_1;F_{2z})} = -\bar{\mu}_y^{(A_1;F_{2x})} = & -\bar{\mu}_z^{(A_1;F_{2y})}, & & & & & & \\
\bar{\mu}_x^{(F_{2x};F_{2y})} = -\bar{\mu}_y^{(F_{2y};F_{2z})} = & -\bar{\mu}_z^{(F_{2x};F_{2z})}, & & & & & & \\
\bar{\mu}_x^{(F_{2z};E_a)} = & 2\bar{\mu}_y^{(F_{2x};E_a)} & = -\frac{2}{\sqrt{3}}\bar{\mu}_y^{(F_{2x};E_b)} = & 2\bar{\mu}_z^{(F_{2y};E_a)} & = \frac{2}{\sqrt{3}}\bar{\mu}_z^{(F_{2z};E_b)}, & & & \\
\bar{\mu}_x^{(F_{2x};F_{1z})} = -\bar{\mu}_x^{(F_{2y};F_{1y})} = & -\bar{\mu}_y^{(F_{2y};F_{1x})} & = & \bar{\mu}_y^{(F_{2y};F_{1z})} & = & \bar{\mu}_z^{(F_{2z};F_{1x})} & = -\bar{\mu}_z^{(F_{2z};F_{1y})}, & \\
\bar{\mu}_x^{(F_{1x};E_b)} = \frac{2}{\sqrt{3}}\bar{\mu}_y^{(F_{1y};E_a)} = & 2\bar{\mu}_y^{(F_{1y};E_b)} & = -\frac{2}{\sqrt{3}}\bar{\mu}_z^{(F_{1z};E_a)} & = 2\bar{\mu}_z^{(F_{1z};E_b)}, & & & &
\end{array} \tag{24}$$

where indices i, f are omitted for simplicity. Therefore Tables 1–3 list only one value for each pair of states. A complete list of 47861 vibrational transition moments and matrix elements

$\bar{\mu}_\alpha^{(i,\Gamma'_a;f,\Gamma''_b)}$ of $^{12}CH_4$ is provided as supplementary material for all allowed transitions in the frequency range from 0 to 10000 cm^{-1} with lower state energies below 5000 cm^{-1}.

Because of the high symmetry of methane many vibrational transition moments $\bar{\mu}^{if}$ vanish. For example, $\bar{\mu}^{if} \equiv 0$ between A_1 eigenfunctions of the ground vibrational state (GS) and any vibrational states of A_1, A_2, E, and F_1 symmetry. This includes transitions within the GS and the transitions giving rise to the fundamental bands $\nu_1(A_1)$ and $\nu_2(E)$. All these transitions have zero vibrational transition moments and are thus dipole forbidden. Certainly this does not rule out ro-vibrational transitions within these bands although such transitions are often also referred to as 'forbidden'. At a formal level any transitions connecting rotation-vibration states with the correct symmetries are allowed [67, 68]. In practice, centrifugal distortions arising from rotation-vibration interactions can introduce F_2-vibrational contributions into, for example, the GS rotational wavefunctions, thus producing non-zero ro-vibrational line strengths. Conversely, 'allowed' ro-vibrational transitions are based only on non-zero vibrational transition moments $\bar{\mu}_\alpha^{(i,\Gamma'_a;f,\Gamma''_b)}$, such as the ones given in Tables 1–3.

The transition moments presented here can be used to derive the effective dipole moment parameters of $^{12}CH_4$, which are important for modelling intensities of this molecule (see Ref. [47] for the most recent collection of the effective dipole moment parameters). Examples of such an exercise can be found in Refs. [43, 69]. For example, the parameter $V^{0(0,0A1)}_{0000A_1-0001F_2} = 0.098677(88)$ D [47] is in good agreement with our value $\sqrt{3}\bar{\mu}_x^{(\mathrm{g.s.},A_1;\nu_4,F_2)} = 0.098314$ D. Similarly, $V^{0(0,0A1)}_{0000A_1-0010F_2} = 0.094622(47)$ D [47] agrees well with our value $\sqrt{3}\bar{\mu}_x^{(\mathrm{g.s.},A_1;\nu_3,F_2)} = 0.093699$ D (see Table 1). Here $\sqrt{3}$ is a conversion factor associated with the Dyad-GS and Pentad-GS zero-order effective dipole constants in the tensorial representation (see, for example, Refs. [38, 39]). For higher vibrational order parameters the correspondence between our transition moments and effective dipole moment parameters is less straightforward owing to the complexity of the effective dipole moment operators which are usually given in a tensorial representation.

From the transition moments computed we also generated vibrational band intensities as given by Brown et al. [38] and [39]:

$$S_{\mathrm{vib}} = \frac{8\pi^3 10^{-36}}{3hcQ_v}\frac{LT_0}{T}e^{-E_\mathrm{i}/kT}\nu_{if}\left(1-e^{-hc\nu_{if}/kT}\right)\bar{\mu}^2_{if}, \tag{25}$$

where ν_{if} and E_i are the vibrational transition frequency and the lower state energy, respectively, Lochschmidt's number $L = 2.686754\times10^{19}$ cm^{-3}, $T_0 = 273.15$ K, k is the Boltzmann constant, and $Q_v = 1.002$ is the vibrational partition function for $T = 278.15$ K. Some of the computed values of S_{vib} are also illustrated in Tables 1–3, where they are compared to the experimental band intensities from Refs. [39, 39, 42, 45–47], where available. The agreement is generally very good. In some cases, particularly for combinational bands, there is some ambiguity over how

to distribute the individual lines between transitions with the same normal-mode vibrational quantum numbers (see also footnotes to Tables 1–3). This introduces an extra uncertainty into these comparisons.

As an illustration of a possible application of our transition moments, Fig. 1 shows the vibrational band intensities calculated at $T = 298.15$ K (empty blue squares) and $T = 1500$ K (filled red circles) using Eq. (25) ($Q_v = 3.038$ at $T = 1500$ K).

6. Conclusion

In this work we present a new *ab initio* DMS for CH_4 which is used to generate the vibrational transition moments and band intensities of $^{12}CH_4$ for a large number of vibrationally allowed transitions. These values should be helpful for predicting intensities for individual bands. The dipole matrix elements can also be used for predicting or evaluating effective dipole moment parameters. The analytical representations for the electric dipole moment and potential energy functions of CH_4 developed in this work have correct symmetry properties of the $T_d(M)$ group and should be useful for representing similar objects obtained using different methods or levels of theory.

Comparisons of calculated and experimental (or experimentally derived) band intensities demonstrate the good quality of our new DMS of CH_4. We are planning to use this DMS in calculations of a high temperature line list for methane within the framework of the ExoMol project [70] (see *www.exomol.com*), which has identified methane as a key target species. Such a line list will be important for modelling molecular opacity in atmospheres of (exo-)planets and cool stars.

Acknowledgments

This work is supported by ERC Advanced Investigator Project 267219 and by the UK Science and Facilities Research Council (STFC).

Table 1: Vibrational transition moments, $\bar{\mu}^{if}$ in D, individual matrix elements $\bar{\mu}_x^{(i,A_1;f,F_{2z})}$ (D), and band intensities, S_{if} in $\mathrm{cm}^{-1}\mathrm{atm}^{-2}$, for $^{12}CH_4$ for transitions from the vibrationally ground state. The calculated and experimentally derived term values $\bar{E}_\mathrm{f}$ of the upper states are given in cm^{-1}.

Γ	State-f	$\bar{E}_\mathrm{f}^\mathrm{obs}$	$\bar{E}_\mathrm{f}^\mathrm{calc}$	$\bar{\mu}_x^{(i,A_1;f,F_{2z})}$	$\bar{\mu}_\mathrm{calc}^{if}$	$S_{if}^{(\mathrm{calc})}$	$S_{if}^{(\mathrm{obs})}$[47]
F_2	0 0 0 1	1310.76	1310.87	-0.05676	0.09831	129.323	127.68
F_2	0 0 0 2	2614.26	2614.32	0.00408	0.00706	1.334	1.05
F_2	0 1 0 1	2830.32	2830.28	0.01038	0.01797	9.346	6.63[a]
F_2	0 0 1 0	3019.49	3019.49	-0.05410	0.09370	271.062	269.92
F_2	0 0 0 3	3870.49	3870.49	-0.00231	0.00401	0.636	0.59 } [b]
F_2	0 0 0 3	3930.92	3930.81	0.00166	0.00288	0.332	0.14 }
F_2	0 1 0 2	4142.86	4142.99	-0.00171	0.00295	0.370	0.34
F_2	1 0 0 1	4223.46	4223.52	0.00775	0.01343	7.791	7.84
F_2	0 0 1 1	4319.21	4319.43	-0.00919	0.01593	11.201	10.24
F_2	0 2 0 1	4348.72	4348.97	-0.00145	0.00252	0.281	0.55 } [c]
F_2	0 2 0 1	4378.95	4379.15	-0.00013	0.00023	0.002	0.23 }
F_2	0 1 1 0	4543.76	4543.90	0.00392	0.00678	2.138	1.26[d]
F_2	0 0 0 4	5143.24	5143.25	0.00035	0.00060	0.019	0.01[e]
F_2	0 0 0 4	5211.29	5210.65	-0.00021	0.00037	0.007	
F_2	0 1 0 3	5370.52	5370.37	-0.00014	0.00023	0.003	
F_2	0 1 0 3	5429.58	5429.07	-0.00058	0.00101	0.056	
F_2	0 1 0 3	5445.12	5444.87	0.00011	0.00020	0.002	
F_2	1 0 0 2		5519.47	0.00011	0.00019	0.002	
F_2	0 0 1 2	5588.03	5586.76	0.00156	0.00270	0.416	
F_2	0 0 1 2		5620.63	-0.00074	0.00129	0.095	
F_2	0 0 1 2		5633.69	-0.00102	0.00176	0.179	
F_2	0 2 0 2	5643.45	5643.64	0.00005	0.00009	0.000	
F_2	0 2 0 2	5668.60	5668.70	-0.00027	0.00047	0.013	
F_2	1 1 0 1		5727.16	0.00016	0.00028	0.005	
F_2	0 1 1 1	5823.10	5823.03	-0.00213	0.00368	0.808	
F_2	0 1 1 1	5844.00	5843.72	-0.00052	0.00089	0.048	
F_2	1 0 1 0		5861.92	-0.00031	0.00054	0.018	
F_2	0 3 0 1	5867.66	5868.23	-0.00026	0.00046	0.012	
F_2	0 3 0 1	5894.12	5894.54	-0.00007	0.00013	0.001	
F_2	0 0 2 0	6004.69	6004.45	-0.00301	0.00522	1.671	1.63[e]
F_2	0 2 1 0	6054.64	6054.67	-0.00055	0.00094	0.055	
F_2	0 2 1 0	6065.32	6065.26	-0.00055	0.00095	0.056	

[a] The total intensity of the $\nu_2+\nu_4$ band, 9.94 $\mathrm{cm}^{-1}\mathrm{atm}^{-2}$ Albert et al. [47], which includes both F_1 and F_2 sub-components agrees well with our $S_{0101F_2}^{(\mathrm{calc})}$ value.

[b] The total intensity of the $3\nu_4$ band, 0.83 $\mathrm{cm}^{-1}\mathrm{atm}^{-2}$ Albert et al. [47], which includes A_1 and F_1 sub-components in addition to two F_2 ones can be compared to the sum of the two 'calc' band intensities $S_{0003F_2}^{(\mathrm{calc})}$.

[c] The total intensity of the $2\nu_2+\nu_4$ band which includes three sub-bands (F_1, F_2 and F_2) by Albert et al. [47] is 0.93 $\mathrm{cm}^{-1}\mathrm{atm}^{-2}$. Hilico et al. [45] reported somewhat smaller value of 0.63 $\mathrm{cm}^{-1}\mathrm{atm}^{-2}$, which suggests a better agreement with our value for the F_2 sub-band only.

[d] Compare to the estimate by Hilico et al. [39], 1.84 $\mathrm{cm}^{-1}\mathrm{atm}^{-2}$, which is closer to our value.

[e] As estimated by Robert et al. [46].

Table 2: Vibrational transition moments, $\bar{\mu}^{if}$ in D, individual matrix elements $\bar{\mu}_x^{(i,\Gamma_\alpha;f,F_{2\beta})}$ ($\alpha = x, y, z$ or a, b and $\beta = x, y, z$) in D, and band intensities, S_{if} in $\mathrm{cm}^{-1}\mathrm{atm}^{-2}$, for $^{12}CH_4$ for the transitions from the ν_4 state. The calculated and experimentally derived term values $\bar{E}_\mathrm{f}$ of the upper states are given in cm^{-1}.

Γ_f	State-f	$\bar{E}_\mathrm{f}^\mathrm{obs}$	$\bar{E}_\mathrm{f}^\mathrm{calc}$	$\bar{\mu}_x^{(i,\Gamma_\alpha;f,F_{2\beta})}$	α	β	$\bar{\mu}_\mathrm{calc}^{if}$	$S_{if}^{(\mathrm{calc})}$	$S_{if}^{(\mathrm{obs})}$[42]
E	0 1 0 0	1533.33	1533.39	-0.00406	a	z	0.00704	0.00013	
A_1	0 0 0 2	2587.04	2586.98	0.05046		z	0.08741	0.17802	
F_2	0 0 0 2	2614.26	2614.32	0.05718	y	x	0.14006	0.46701	0.931^a
E	0 0 0 2	2624.62	2624.61	0.06530	a	z	0.11310	0.30697	
F_2	0 1 0 1	2830.32	2830.28	0.00641	y	x	0.01569	0.00684	0.00872
F_1	0 1 0 1	2846.07	2846.06	0.00007	z	x	0.00016	0.000001	
A_1	1 0 0 0	2916.48	2916.54	0.00236		z	0.00408	0.00049	0.000689
F_2	0 0 1 0	3019.49	3019.49	-0.01675	a	z	0.04104	0.05265	0.0481
A_1	0 2 0 0	3063.65	3063.61	-0.00088		z	0.00153	0.00007	0.0005
E	0 2 0 0	3065.14	3065.12	0.00144	a	z	0.00250	0.00020	
F_2	0 0 0 3	3870.49	3870.49	-0.00383	a	z	0.00938	0.00412	
A_1	0 0 0 3	3909.20	3909.68	-0.00424		z	0.00734	0.00256	
F_1	0 0 0 3	3920.51	3920.15	-0.00320	z	x	0.00784	0.00293	
F_2	0 0 0 3	3930.92	3930.81	-0.00299	a	z	0.00732	0.00257	
E	0 1 0 2	4101.39	4101.49	-0.00973	a	z	0.01685	0.01451	
F_1	0 1 0 2	4128.76	4128.73	0.00890	z	x	0.02180	0.02451	
A_1	0 1 0 2	4132.86	4132.83	0.00923		z	0.01599	0.01320	
F_2	0 1 0 2	4142.86	4142.99	-0.00537	a	z	0.01315	0.00897	
E	0 1 0 2	4151.21	4151.28	0.00525	a	z	0.00910	0.00430	
F_2	1 0 0 1	4223.46	4223.52	0.00244	a	z	0.00597	0.00190	
F_2	0 0 1 1	4319.21	4319.43	-0.03798	a	z	0.09303	0.47649	
E	0 0 1 1	4322.18	4322.21	-0.04272	a	z	0.07399	0.30170	
A_1	0 0 1 1	4322.70	4322.40	-0.03326		z	0.05761	0.18292	
F_1	0 0 1 1	4322.59	4322.66	-0.03760	z	x	0.09211	0.46758	
F_2	0 2 0 1	4348.72	4348.97	-0.00451	a	z	0.01104	0.00678	
F_1	0 2 0 1	4363.61	4363.61	0.00076	z	x	0.00186	0.00019	
F_2	0 2 0 1	4378.95	4379.15	-0.00057	a	z	0.00140	0.00011	
E	1 1 0 0	4435.12	4435.18	-0.00095	a	z	0.00165	0.00015	
F_1	0 1 1 0	4537.55	4537.75	0.00143	z	x	0.00351	0.00073	
F_2	0 1 1 0	4543.76	4543.90	-0.00121	a	z	0.00297	0.00052	
E	0 3 0 0	4592.03	4592.12	-0.00030	a	z	0.00052	0.00002	
A_1	0 3 0 0	4595.51	4595.66	0.00000		z	0.00000	0.00000	

[a] This 'experimental' vibrational intensity of the $2\nu_4$ band [42] correlates with our $S_{0002A_1}^{(\mathrm{calc})} + S_{0002F_2}^{(\mathrm{calc})} + S_{0002E}^{(\mathrm{calc})} = 0.952$ $\mathrm{cm}^{-1}\mathrm{atm}^{-2}$.

Table 3: Vibrational transition moments, $\bar{\mu}^{if}$ in D, individual matrix elements $\bar{\mu}_x^{(i,\Gamma\alpha;f,E_\beta)}$ ($\alpha = x, y, z$ and $\beta = a, b$) in D. and band intensities, S_{if} in $\mathrm{cm}^{-1}\mathrm{atm}^{-2}$, for $^{12}CH_4$ for the transitions from the ν_2 state. The calculated and experimentally derived term values $\bar{E}_\mathrm{f}$ of the upper states are given in cm^{-1}.

Γ_f	State-f	$\bar{E}_\mathrm{f}^\mathrm{obs}$	$\bar{E}_\mathrm{f}^\mathrm{calc}$	$\bar{\mu}_x^{(i,\Gamma\alpha;f,E_\beta)}$	α	β	$\bar{\mu}_\mathrm{calc}^{if}$	$S_{if}^\mathrm{(calc)}$	$S_{if}^\mathrm{(obs)}$[42]
F_2	0 0 0 2	2614.26	2614.32	0.00110	z	a	0.00191	0.00002	0.00008
F_2	0 1 0 1	2830.32	2830.28	-0.05740	z	a	0.09942	0.08000	0.145^a
F_1	0 1 0 1	2846.07	2846.06	-0.05718	x	b	0.09904	0.08037	
F_2	0 0 1 0	3019.49	3019.49	-0.01835	z	a	0.03178	0.00938	0.0085
F_2	0 0 0 3	3870.49	3870.49	0.00030	z	a	0.00052	0.000004	
F_1	0 0 0 3	3920.51	3920.15	-0.00034	x	b	0.00058	0.000005	
F_2	0 0 0 3	3930.92	3930.81	-0.00010	z	a	0.00017	0.0000005	
F_1	0 1 0 2	4128.76	4128.73	-0.00367	x	b	0.00636	0.00066	
F_2	0 1 0 2	4142.86	4142.99	-0.00292	z	a	0.00507	0.00042	
F_2	1 0 0 1	4223.46	4223.52	-0.00310	z	a	0.00536	0.00048	
F_2	0 0 1 1	4319.21	4319.43	-0.00142	z	a	0.00245	0.00010	
F_1	0 0 1 1	4322.59	4322.66	-0.00218	x	b	0.00377	0.00025	
F_2	0 2 0 1	4348.72	4348.97	0.01360	z	a	0.02355	0.00977	
F_1	0 2 0 1	4363.61	4363.61	-0.01117	x	b	0.01934	0.00662	
F_2	0 2 0 1	4378.95	4379.15	-0.00081	z	a	0.00139	0.00003	
F_1	0 1 1 0	4537.55	4537.75	-0.05404	x	b	0.09360	0.16459	
F_2	0 1 1 0	4543.76	4543.90	0.05344	z	a	0.09255	0.16125	
F_2	0 0 0 4	5143.24	5143.25	-0.00007	z	a	0.00011	0.00000	
F_2	0 0 0 4	5211.29	5210.65	-0.00011	z	a	0.00019	0.00000	
F_1	0 0 0 4	5230.78	5230.07	0.00003	x	b	0.00005	0.00000	
F_2	0 1 0 3	5370.52	5370.37	-0.00262	z	a	0.00454	0.00049	
F_1	0 1 0 3	5389.67	5389.71	0.00191	x	b	0.00331	0.00026	
F_2	0 1 0 3	5429.58	5429.07	0.00117	z	a	0.00202	0.00010	
F_1	0 1 0 3	5436.79	5436.50	0.00102	x	b	0.00176	0.00008	
F_2	0 1 0 3	5445.12	5444.87	-0.00064	z	a	0.00110	0.00003	
F_1	0 1 0 3	5462.92	5462.74	0.00198	x	b	0.00343	0.00029	

[a] This 'experimental' vibrational intensity of the $\nu_2 + \nu_4$ band [42] correlates with our $S_{0101F_1}^\mathrm{(calc)} + S_{0101F_2}^\mathrm{(calc)} = 0.160$ $\mathrm{cm}^{-1}\mathrm{atm}^{-2}$.

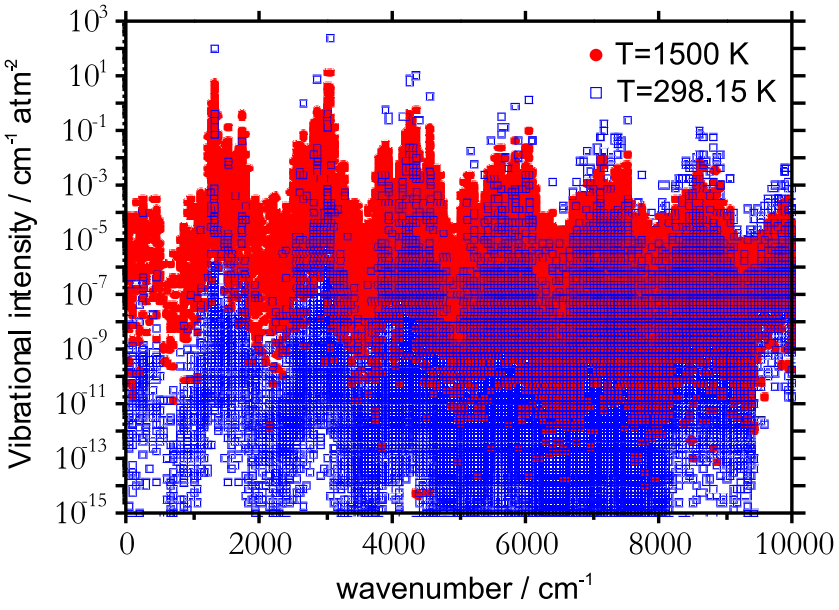

Figure 1: Vibrational band intensities calculated at $T = 298.15$ K (filled blue circles) and $T = 1500$ K (empty red squares) using Eq. (25).

References

[1] B. M. Dinelli, S. Miller, N. Achilleos, H. A. Lam, M. Cahill, J. Tennyson, M. F. Jagod, T. Oka, J. C. Hilico, T. R. Geballe, Icarus 126 (1997) 107–125.

[2] M. R. Swain, G. Vasisht, G. Tinetti, Nature 452 (2008) 329–331.

[3] J. P. Beaulieu, G. Tinetti, D. Kipping, I. Ribas, R. J. Barber, J. Y.-K. Cho, I. Polichtchouk, J. Tennysson, S. N. Yurchenko, C. A. Griffith, I. Waldmann, S. Miller, S. Carey, O. Mousis, S. J. Fossey, A. Aylward, Astrophys. J. 731 (2011) 16.

[4] T. R. Geballe, S. R. Kulkarni, C. E. Woodward, G. C. Sloan, Astrophys. J. 467 (1996) L101–L104.

[5] R. J. Duchovic, W. L. Hase, H. B. Schlegel, J. Chem. Phys. 88 (1984) 1339–1347.

[6] T. J. Lee, J. M. L. Martin, P. R. Taylor, J. Chem. Phys. 102 (1995) 254–261.

[7] D. W. Schwenke, H. Partridge, Spectra Chimica Acta A 57 (2001) 887–895.

[8] R. Marquardt, M. Quack, J. Phys. Chem. A 108 (2004) 3166–3181.

[9] C. Oyanagi, K. Yagi, T. Taketsugu, K. Hirao, J. Chem. Phys. 124 (2006) 064311.

[10] A. V. Nikitin, M. Rey, V. G. Tyuterev, Chem. Phys. Lett. 501 (2011) 179–186.

[11] R. Warmbier, R. Schneider, A. R. Sharma, B. J. Braams, J. M. Bowman, P. H. Hauschildt, Astron. Astrophys. 495 (2009) 655–661.

[12] H. Hollenstein, R. R. Marquardt, M. Quack, M. A. Suhm, J. Chem. Phys. 101 (1994) 3588–3602.

[13] S. N. Yurchenko, W. Thiel, P. Jensen, J. Mol. Spectrosc. 245 (2007) 126–140.

[14] S. N. Yurchenko, M. Carvajal, A. Yachmenev, W. Thiel, P. Jensen, J. Quant. Spectrosc. Radiat. Transf. 111 (2010) 2279–2290.

[15] R. I. Ovsyannikov, W. Thiel, S. N. Yurchenko, M. Carvajal, P. Jensen, J. Chem. Phys. 129 (2008) 044309.

[16] A. Yachmenev, S. N. Yurchenko, P. Jensen, O. Baum, T. F. Giesen, W. Thiel, Phys. Chem. Chem. Phys. 12 (2010) 8387–8397.

[17] A. Yachmenev, S. N. Yurchenko, P. Jensen, W. Thiel, J. Chem. Phys. 134 (2011) 244307.

[18] A. Yachmenev, S. N. Yurchenko, T. Ribeyre, W. Thiel, J. Chem. Phys. 135 (2011) 074302.

[19] S. N. Yurchenko, R. J. Barber, J. Tennyson, Mon. Not. R. Astr. Soc. 413 (2011) 1828–1834.

[20] D. Underwood, J. Tennyson, S. Yurchenko, Phys. Chem. Chem. Phys, submitted (2013).

[21] O. Polyansky, I. Kozin, P. Maĺyszek, J. Koput, J. Tennyson, S. Yurchenko, J. Phys. Chem. A, submitted (2013).

[22] X. G. Wang, T. Carrington, J. Chem. Phys. 121 (2004) 2937–2954.

[23] X. G. Wang, T. Carrington, J. Chem. Phys. 119 (2003) 101–117.

[24] X. G. Wang, T. Carrington, J. Chem. Phys. 118 (2003) 6946–6956.

[25] X. G. Wang, T. Carrington, J. Chem. Phys. 118 (2003) 6260–6263.

[26] S. Carter, H. M. Shnider, J. M. Bowman, J. Chem. Phys. 110 (1999) 8417–8423.

[27] S. Carter, J. M. Bowman, J. Phys. Chem. A 104 (2000) 2355–2361.

[28] J. Wu, X. Huang, S. Carter, J. M. Bowman, Chem. Phys. Lett. 426 (2006) 285–289.

[29] A. Chakraborty, D. G. Truhlar, J. M. Bowman, S. Carter, J. Chem. Phys. 121 (2004) 2071–2084.

[30] E. Mátyus, G. Czakó, A. G. Császár, J. Chem. Phys. 130 (2009) 134112.

[31] L. Halonen, J. Chem. Phys. 106 (1997) 831–845.

[32] J. Xie, J. Tennyson, Mol. Phys. 100 (2002) 1615–1622.

[33] D. W. Schwenke, Spectra Chimica Acta A 58 (2002) 849–861.

[34] A. V. Nikitin, Opt. Spectrosc. 106 (2009) 176–182.

[35] H. G. Yu, J. Chem. Phys. 121 (2004) 6334–6340.

[36] H.-G. Yu, J. Mol. Spectrosc. 256 (2009) 287–298.

[37] J. C. Hilico, M. Loete, L. R. Brown, J. Mol. Spectrosc. 111 (1985) 119–137.

[38] L. R. Brown, M. Loëte, J. Hilico, J. Mol. Spectrosc. 133 (1989) 273–311.

[39] J. C. Hilico, M. Loëte, L. R. Brown, J. Mol. Spectrosc. 152 (1992) 229–251.

[40] J. C. Hilico, G. S. Baronov, D. K. Bronnikov, S. A. Gavrikov, I. I. Nikolaev, V. D. Rusanov, Y. G. Filimonov, J. Mol. Spectrosc. 161 (1993) 435–444.

[41] J. C. Hilico, J.-P. Champion, S. Toumi, V. G. Tyuterev, S. A. Tashkun, J. Mol. Spectrosc. 168 (1994) 455–476.

[42] O. Ouardi, J. C. Hilico, M. Loëte, L. R. Brown, J. Mol. Spectrosc. 180 (1996) 311–322.

[43] A. Mourbat, A. Aboumajd, M. Loete, J. Mol. Spectrosc. 190 (1998) 198–212.

[44] L. Fejard, J.-P. Champion, J. M. Jouvard, L. R. Brown, A. S. Pine, J. Mol. Spectrosc. 201 (2000) 83–94.

[45] J. C. Hilico, O. Robert, M. Loëte, S. Toumi, A. S. Pine, L. R. Brown, J. Mol. Spectrosc. 208 (2001) 1–13.

[46] O. Robert, J. C. Hilico, M. Loëte, J.-P. Champion, L. R. Brown, J. Mol. Spectrosc. 209 (2001) 14–23.

[47] S. Albert, S. Bauerecker, V. Boudon, L. R. Brown, J. P. Champion, M. Loëte, A. Nikitin, M. Quack, Chem. Phys. 356 (2009) 131–146.

[48] T. B. Adler, G. Knizia, H.-J. Werner, J. Chem. Phys. 127 (2007) 221106.

[49] K. A. Peterson, T. B. Adler, H.-J. Werner, J. Chem. Phys. 128 (2008) 084102.

[50] H. J. Werner, P. J. Knowles, R. Lindh, F. R. Manby, M. Schütz, et al., MOLPRO, a package of ab initio programs, 2010. See `http://www.molpro.net/`.

[51] S. N. Yurchenko, R. J. Barber, A. Yachmenev, W. Thiel, P. Jensen, J. Tennyson, J. Phys. Chem. A 113 (2009) 11845–11855.

[52] P. R. Bunker, P. Jensen, Molecular Symmetry and Spectroscopy, NRC Research Press, Ottawa, 2 edition,

1998.

[53] O. Alvarez-Bajo, R. Lemus, M. Carvajal, F. Perez-Bernal, Mol. Phys. 109 (2011) 797–812.

[54] S. Yurchenko, M. Carvajal, H. Lin, J. Zheng, W. Thiel, P. Jensen, J. Chem. Phys. 122 (2005) 104317.

[55] H. Partridge, D. W. Schwenke, J. Chem. Phys. 106 (1997) 4618–4639.

[56] J. F. Stanton, Mol. Phys. 97 (1999) 841–845.

[57] L. S. Rothman, I. E. Gordon, A. Barbe, D. C. Benner, P. F. Bernath, M. Birk, V. Boudon, L. R. Brown, A. Campargue, J. P. Champion, et al, J. Quant. Spectrosc. Rad. Transf. 110 (2009) 533–572.

[58] S. N. Yurchenko, R. J. Barber, J. Tennyson, W. Thiel, P. Jensen, J. Mol. Spectrosc. 268 (2011) 123–129.

[59] J. W. Cooley, Math. Comp. 15 (1961) 363–374.

[60] B. Numerov, Mon. Not. R. Astron. Soc. 84 (1924) 592–602.

[61] C. Wenger, J.-P. Champion, J. Quant. Spectrosc. Radiat. Transf. 59 (1998) 471–480.

[62] V. Boudon, M. Rey, M. Loëte, J. Quant. Spectrosc. Radiat. Transf. 98 (2006) 394–404.

[63] A. V. Nikitin, O. M. Lyulin, S. N. Mikhailenko, V. I. Perevalov, N. N. Filippov, I. M. Grigoriev, I. Morino, T. Yokota, R. Kumazawa, T. Watanabe, J. Quant. Spectrosc. Radiat. Transf. 111 (2010) 2211–2224.

[64] C. Eckart, Phys. Rev. 47 (1935) 552–558.

[65] C. R. Le Sueur, S. Miller, J. Tennyson, B. T. Sutcliffe, Mol. Phys. 76 (1992) 1147–1156.

[66] J. Hougen, Methane Symmetry Operations, NIST, Gaithersburg, MD., 2001. Version 1.0 [Online]. Available: `http://physics.nist.gov/Methane`.

[67] S. Miller, J. Tennyson, Astrophys. J. 335 (1988) 486–490.

[68] S. Miller, J. Tennyson, B. T. Sutcliffe, J. Mol. Spectrosc. 141 (1990) 104–117.

[69] V. I. Perevalov, O. M. Lyulin, V. G. Tyuterev, M. Loete, J. Mol. Spectrosc. 149 (1991) 15–33.

[70] J. Tennyson, S. N. Yurchenko, Mon. Not. R. Astr. Soc. 425 (2012) 21–33.